Thermal radiation spectra of individual subwavelength microheaters

Yat-Yin Au,* Helgi Skuli Skulason, and Snorri Ingvarsson†
Science Institute, University of Iceland, Dunhaga 3, Reykjavik IS-107, Iceland

Levente J. Klein and Hendrik F. Hamann
IBM T. J. Watson Research Center, 1102 Kitchawan Road, Yorktown Heights, New York 10598, USA
(Received 1 April 2008; published 1 August 2008)

Polarization resolved spectra of infrared radiation from individual electrically driven platinum microheaters have been measured by Fourier-transform infrared spectrometry as a function of heaters' width. When the heater width approaches zero, the signal with polarization parallel to the heater long axis converges to a finite value, while its perpendicularly polarized counterpart drops below our detection limit. As a result this leads to strongly polarized radiation for very narrow heaters. Further, while the parallel polarized radiation spectra appear to be insensitive to heater width variation (at least within the sensitive range of our light detector), the perpendicular polarized spectra were heavily affected. We observed a $\lambda/2$-like resonance that we attribute to correlation of charge oscillations across the heater's width, which are possibly mediated by surface plasmons. These findings provide implications for fabrication of nanoscale electrically driven thermal antennas.

DOI: 10.1103/PhysRevB.78.085402 PACS number(s): 44.40.+a, 62.23.Hj, 71.45.Gm, 84.40.Ba

Recently there has been great advancement of knowledge on thermal radiation from microstructured surfaces. It has been predicted that propagation of surface waves produces long-range correlation between charge fluctuations at a material's surface.[1] If the surface is appropriately patterned, this results in enhanced coherence of thermal radiation. Such a phenomenon has been observed in periodic structures of dielectric[2] and metallic materials.[3,4] This coherence enhancement in far-field radiation corresponds to a strong near field due to less efficient cancellation of higher order multipole terms.[5] Strongly overlapping near fields of adjacent objects have been theoretically predicted to provide a better heat transfer mechanism than when the same objects are in direct physical contact.[6] This should be very important in thermophotovoltaic (TPV) energy conversion applications, e.g., see Ref. 7. However, instead of exploiting the near field over a large area as in the TPV case, there is also interest in confining this near field to an extremely small region, serving applications such as thermally assisted magnetic recording[8] and near-field optical microscopy.[9] Nanoscale optical antennas have been fabricated to provide local-field enhancement under irradiation of an external light source in the visible and infrared range.[10–13] We, on the other hand, explore another avenue in providing the localized near field, namely, resistive electric current heating ("Ohmic" heating) of metallic microwires.[14] Although we do not probe the near field directly in this work we can use the far-field radiative properties of the microwires, which lie mostly in the midinfrared, to shed light on fabrication of an electrically driven near-field infrared local source.[15]

The effects of the size and shape of a thermal source on its radiation properties are not thoroughly understood when its dimension approaches the wavelength of the radiation. Standing waves of thermally generated charge oscillations in the near field have recently been observed across metallic stripes with width on the order of tens of microns.[16] Since a surface plasmon propagates only in the direction of charge oscillation,[1] one would expect charge oscillations to be affected differently depending on whether they are parallel or perpendicular to the heater axis as the heater's width is narrowed down. When the width approaches the length scale of these surface charge oscillations, one might expect a modification in radiation to result. In this paper, we performed a systematic study of thermal radiation from metallic wires with constant length and various widths, with detected radiation resolved in polarization oriented parallel and perpendicular to the wire long axis (from now on, we will abbreviate the two polarizations as "parallel" and "perpendicular"). We typically refer to the wires as heaters, as we electrically heat them to induce thermal radiation.

Platinum microwires with length (thickness) fixed at 8 μm (50 nm) and width varied from 8 to 0.05 μm have been fabricated on Si/SiO_2 (150 nm) substrate using standard electron-beam lithography, dc sputtering, and lift-off technique. To improve adhesion we deposited 10 nm of titanium underneath the platinum. Figure 1(a) shows the scanning electron microscope (SEM) image for an 8×0.8 μm^2

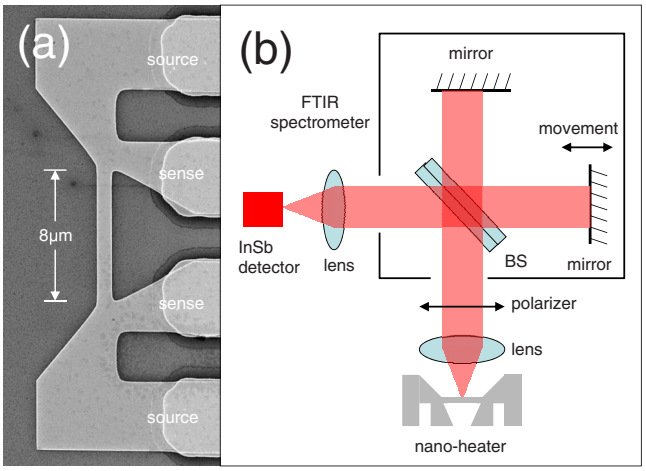

FIG. 1. (Color online) (a) SEM image of an 8×0.8 μm^2 microheater. (b) Schematics for the experiment. Radiation emitted by the nanoheater is analyzed with the FTIR system.

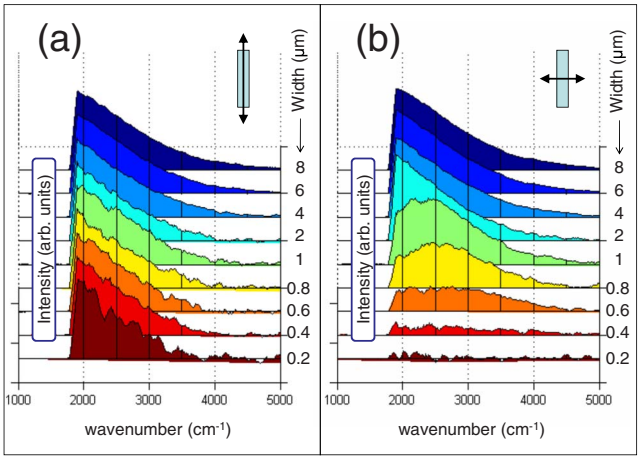

FIG. 2. (Color online) FTIR spectra obtained from heaters at a temperature of 750 K. (a) For polarization parallel to heater long axis. (b) For polarization perpendicular to heater long axis. Numbers next to each spectrum on the right side indicate the corresponding heater width in microns. For each width, spectra for both polarization directions are divided by the same normalization factor in order to align peaks for different widths in the parallel polarization case to the same height.

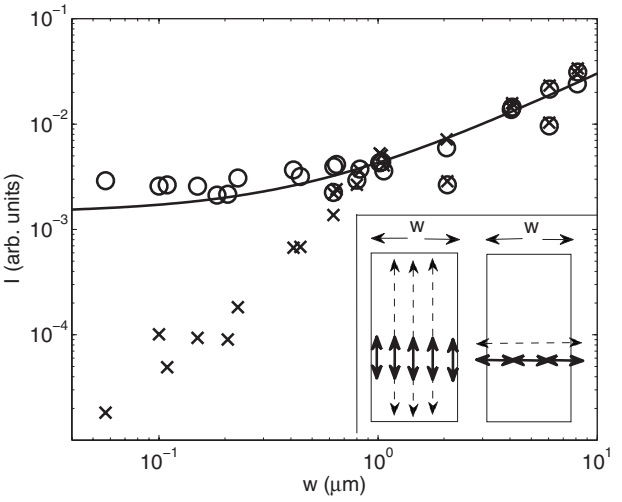

FIG. 3. Integrated intensity (I) from 2000 to 3500 cm^{-1} of the FTIR spectra in Fig. 2 against heaters width (w). The polarization direction is parallel (circles) and perpendicular (crosses) to the heater long axis. The solid line shows the best linear fit to the parallel polarization data. Inset: illustrations of radiating dipoles and surface plasmons across the heater's width. The two rectangular boxes represent the same microheater, viewed from above the sample surface. The horizontal and vertical boundaries of the boxes represent the width and length of the heater, respectively. Short solid arrows within the two boxes represent oscillating dipoles for parallel (left box) and perpendicular (right box) polarizations, respectively. Long dashed arrows represent the propagation direction of corresponding surface plasmons.

heater. The four-wire configuration allows heating of the wire by passing an electrical current through the two source wires while at the same time monitoring the resistance through the two sensing wires, thus allowing us to maintain the heater at desired power using a feedback mechanism. In an independent study, it has been established that although the resistance-temperature relationship of these metallic heaters can be influenced by the annealing effect of high currents, the relationship between applied power and temperature rise in the heater remains unaltered. Therefore by keeping the applied power constant, we are able to maintain the temperature of the heater at a desired value.

As illustrated in Fig. 1(b), a single electrically driven heater is brought into focus with a reflective objective (numerical aperture equals 0.5 and focal length of 5.41 mm). The collected infrared light is analyzed by a polarizer before entering a Fourier-transform infrared (FTIR) spectrometer. The resulting optical signal is detected by a liquid nitrogen cooled InSb detector. Figure 2 presents spectral data obtained as a function of heater width for (a) parallel and (b) perpendicular polarizations, with heater temperature fixed at 750 K. These spectra have been corrected to take into account the spectral response of the FTIR system plus related optics, obtained by calibration with a SiC thermal source.[17] For each given wire width in Fig. 2, spectra for both polarization orientations are normalized with the same numerical factor. These factors are chosen to align the intensity of the peaks for different width samples in the *parallel polarized* case [Fig. 2(a)] to the same height (therefore data of different width have different normalizing factors). This is purely for visualization purposes. All the spectra share a sharp cutoff at roughly 1800 cm^{-1} due to the spectral response of our InSb detector. At 750 K, thermal blackbody radiation peaks at an energy below this cutoff. Therefore only the tails of such spectra are accessible to us. Also, for an ideal blackbody the Planck spectrum depends only on temperature. As we can see in Fig. 2(a), for parallel polarization the shape of the tails is largely unchanged for different wire widths. The only apparent difference between the spectra is a slightly faster decay of the tail at the high wave-number end as the heater width decreases. In contrast, there is a dramatic modification of our spectra with perpendicular polarization [Fig. 2(b)]. The onset of these changes occurs at a wire width of $w=1$ μm. At widths $w \geq 2$ μm the spectra for both polarizations are almost identical. However, as the widths are decreased to 1 and 0.8 μm the peak shifts from the $w>2$ μm value of below 1800 cm^{-1} (inaccessible to us) to roughly 2500 cm^{-1}. The shift of the peak is accompanied with a decrease in the overall intensity, and eventually it falls below our sensitivity limit once the width reaches 0.2 μm.

A summary of intensity of the above-mentioned spectra integrated over the energy range from 2000 to 3500 cm^{-1} against heater width is displayed in Fig. 3. Circles and crosses represent parallel and perpendicular polarizations, respectively. Intensities for both polarizations dropped from 3×10^{-2} at $w=8$ μm to 4×10^{-3} at $w=1.0$ μm. Although intensities from different individual heaters of certain intermediate width values (notably $w=2$ and 6 μm) were not as reproducible as others for unknown reasons, a general trend of decreasing intensity with narrowing width from $w=8$ μm to $w=1$ μm is still recognizable. This agrees with common sense that the total radiation should scale with the heater surface area. If the heater's width (i.e., surface area) decreases, then so should the radiation intensity.

However, as heater's width decreases further below 1 μm, integrated intensities for parallel polarization *consistently* stabilize at a finite value around 3×10^{-3}. This lack of dependence of intensity on width for $w<1$ μm is an important finding of this research work which indicates that at these length scales, the heater's surface area is no longer the dominating factor in determining radiation intensity for the parallel polarization. At the same time the intensity of the corresponding perpendicular polarization signal continues to decrease with heater width in this $w<1$ μm region. This results in strongly polarized emission for microheaters with width smaller than 0.2 μm as observed previously.[14,18]

To gain further insight into our observations we turn to a simple model of the radiated signal intensity. We assume the thermal radiation at frequency ω to originate from individual microscopic and indivisible electric dipole oscillators with natural oscillation frequency ω, with fixed position evenly distributed across the heater's metallic surface. These dipoles are assumed to be either aligned parallel or perpendicular to the heater long axis (Fig. 3, inset) and are continuously stimulated by the thermal environment, resulting in radiation with polarization in the parallel or perpendicular direction, respectively. Observing the radiation far enough away from the heater, all oscillating dipoles on the heater surface are virtually located at the same point in space from the observer's point of view. Therefore these dipoles contribute to the optical electric field E at the observer's position on equal footing. Assuming the ith dipole located at $\mathbf{r}_i$ on the heater surface is oscillating with an amplitude $P(\mathbf{r}_i)$, then for each radiation polarization, the intensity I is simply given by

$$I=\langle|E|^2\rangle=\left\langle\left|\sum_i P(\mathbf{r}_i)\right|^2\right\rangle=\sum_{i,j}\langle P^*(\mathbf{r}_i)P(\mathbf{r}_j)\rangle, \qquad (1)$$

where angular brackets denote time averaging. The calculation of intensity is thus reduced to a summation of the dipole correlation function $\langle P^*(\mathbf{r})P(\mathbf{r}')\rangle$ over all possible discretized values of $\mathbf{r}$ and $\mathbf{r}'$ on the heater surface.

The above-mentioned individual dipoles, driven by their local thermal environment, should in principle oscillate independently from each other [i.e., $\langle P^*(\mathbf{r})P(\mathbf{r}')\rangle\propto\delta(\mathbf{r}-\mathbf{r}')$]. However, under certain circumstances, the heater surface supports collective vibrational modes of these dipoles, i.e., surface plasmons, which strongly affect the dipole correlation function. Since a surface plasmon travels largely parallel to the direction of charge oscillation,[1] this sheds light on the different width dependences of the intensity data from the two different polarization directions in the region of $w<1$ μm in Fig. 3. Radiation with parallel (perpendicular) polarization originates from charge oscillation parallel (perpendicular) to the heater's long axis. Thus across the width of the heater, dipole oscillations resulting in parallel polarized radiation do not enjoy communication by surface plasmons (left box of Fig. 3, inset) and therefore correlation between these dipoles is minimal, whereas dipole oscillations resulting in perpendicular polarization are communicated by surface plasmons (right box of Fig. 3, inset) and are therefore strongly correlated. We therefore expect radiation with parallel and perpendicular polarizations to respond quite differently when the heater width varies. Obviously this will also show up as a modification in their intensity ratio.

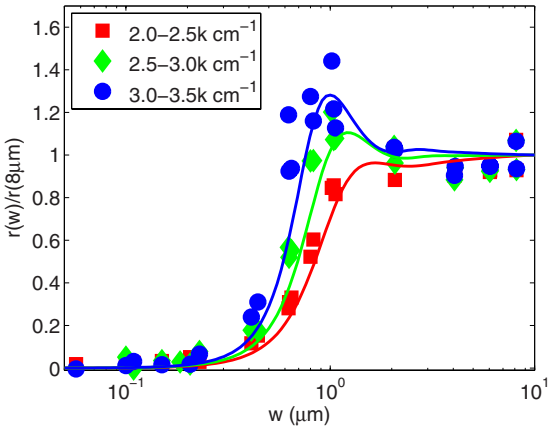

FIG. 4. (Color online) Reduced intensity ratio (data normalized with the value at 8 μm) versus heater width for averaged value in the windows of 2000–2500 (red squares), 2500–3000 (green diamonds), and 3000–3500 (blue circles) cm^{-1}. The solid curves are best fits based on our model (see text) for wave numbers 2250 (red), 2750 (green), and 3250 (blue) cm^{-1}.

Let us define the intensity ratio as $r=I_{\text{perp}}/I_{\text{para}}$, where I_{perp} and I_{para} represent the signal intensity for perpendicular and parallel polarizations, respectively. Let us further define the reduced intensity ratio at a given width w as $r(w)$ divided by r ($w=8$ μm). Figure 4 presents experimental data of the reduced intensity ratio averaged over three different spectral windows: 2000–2500 (red), 2500–3000 (green), and 3000–3500 (blue) cm^{-1}. While for all three windows, data points start out at 1.0 in the wide heater limit ($w>2.0$ μm) and end up approaching zero in the narrow-width limit ($w<0.2$ μm), the different spectral windows do exhibit different trends in the intermediate region (0.2 μm $<w<2.0$ μm). When w decreases starting from the broad limit, the 2000–2500 cm^{-1} data drop at earlier heater width than the 2500–3000 cm^{-1} ones, which in turn drop sooner than the 3000–3500 cm^{-1} data. This is another manifestation of the same behavior as in the shift of spectral peak to higher wave number we saw in Fig. 2(b) in the intermediate width region ($w=1.0$, 0.8, and 0.6 μm). Moreover, data tend to demonstrate a resonancelike bump immediately before attenuation, with the data from the higher wave-number window showing a more prominent bump (the obvious rise of data points for the 3000–3500 cm^{-1} window around the $w=1.0$ μm position).

In order to provide a physical picture behind these frequency dependences, we turn again to our aforementioned dipole correlation function in Eq. (1). Suppose a one-dimensional case. Since for the perpendicular polarized case correlation between dipoles across the heater width is likely to be mediated by surface plasmons, we assume the correlation function to take the form $\langle P^*(x)P(x')\rangle=\Theta(\omega,T)f(x-x')$, where

$$f(x)=\exp\left(-\frac{|x|}{d}\right)\cos\left(\frac{2\pi x}{\lambda}\right), \qquad (2)$$

where λ is the wavelength of the corresponding surface plasmon for a particular wave number of radiation, related to the

electromagnetic wave in free space with wavelength λ_{free} as $\lambda=\lambda_{free}/n$. n is the effective refractive index for the surface wave and d represents the decay length for this correlation. By assuming a penetration depth of $\lambda/2\pi$ and taking average between the free space above and the substrate below, we determine $n=1.665$. The function $f(x)$ resembles a traveling plasmonic wave with attenuation. We assume that $\Theta(\omega,T)$ is a function that describes the frequency (ω) and temperature (T) dependence of the dipole correlation function. Because Θ lacks dependence in positions x and x', its contribution is removed upon division of $r(w)$ with $r(w=8\ \mu\text{m})$. Therefore it does not enter either in the final result of the reduced intensity ratio's dependence on width. Thus it is only the function $f(x)$ that matters with respect to representation of our data with the reduced intensity ratio. The correlation signal is assume to reflect with 180° phase shift at the two edges and it obeys the principle of superposition, i.e., the surface plasmons are superposable and reflect at physical edge with a phase shift. The overall correlation between x and x' after taking the existence of edges into account becomes

$$f(x,x') = \sum_{n=-\infty}^{\infty} (-1)^n f[x - \hat{M}_n(x')], \tag{3}$$

where $\hat{M}_n(x')$ denotes the nth image of x' on the two sides behind the edges, i.e.,

$$\hat{M}_n(x') = wn + (-1)^n x'. \tag{4}$$

The heater is assumed to be located within $x \in [-0.5w, 0.5w]$.

By inserting Eqs. (2)–(4) into Eq. (1), the intensity I_{perp} can be calculated as essentially a convolution problem. The parallel polarization intensity I_{para} is simply obtained by linear fitting the parallel polarization data in Fig. 3. Writing $I_{para}=\alpha w+\beta$, fitting results in $\alpha=0.002\ 88$ and $\beta=0.001\ 43$ (see solid curve in Fig. 3). This way we were able to produce r (equals I_{perp}/I_{para}) and therefore the reduced intensity ratio $[r(w)/r(w=8\ \mu\text{m})]$. A best fit to the data in Fig. 4 was obtained by using $d=0.55\ \mu$m (note that d is the *only* adjustable parameter) and the results are plotted as curves in Fig. 4 for three different wave-number values: 2250 (red), 2750 (green), and 3250 (blue) cm^{-1}, which are the median values of the three spectral windows defined above. As we can see, the simulation satisfactorily reproduces the experimental frequency dependence characteristics, with lower wave-number values dropping sooner than the higher ones as width w decreases. The bump's dependence on wave number was also reproduced satisfactorily, with it hardly visible for 2250 cm^{-1}, while for 3250 cm^{-1} it rises to roughly 1.3, notably above the value of 1.0 in the case of the widest heaters.

The above analysis is by no means a rigorous representation of the real physical system. However, our simple model seems to capture the essential features providing a very satisfying agreement between simulation and experimental data. It also provides certain physical insight, especially into how surface plasmons play an important role in the observed variation of intensity with heater width. In Fig. 4, the bump occurring around 1.0 μm for the 3000–3500 cm^{-1} window represents a $\lambda/2$ resonance. The effective wavelength is shorter than its free space counterpart, taking into account of the slower traveling speed of surface plasmons.

In conclusion, we have obtained spectral and intensity dependence of microheaters on their width at a fixed length, within the spectral sensitive range of our InSb detector. The result is strongly polarization dependent and is explained in the context of correlation of charge oscillations across the heater's width. For parallel polarization, we found that intensity converges to a finite value as heater width approaches zero, implying that heater surface area is no longer a determining factor for radiation with parallel polarization in this subwavelength width scale. This leads to highly polarized radiation at $w<200$ nm since the corresponding radiation with perpendicular polarization diminishes at these widths. For perpendicular polarization, we found a strong width dependence in the intermediate width region of $0.2\ \mu\text{m}<w<2\ \mu$m. In addition, an antennalike $\lambda/2$ resonance was observed. We explain this in terms of surface wave mediated correlation of dipoles across the heater width. All of these pave the way to fabrication of a thermally driven highly polarized $\lambda/2$ infrared antenna, which would be significant in the physics of near-field optics. The technology is important for tunable infrared emitters with high power in a narrow spectral band, which is important for sensing, spectroscopy, and thermophotovoltaic applications.

This research was funded in part by the Icelandic Research Fund and the University of Iceland Research Fund.

*auyy@hi.is
†sthi@hi.is

[1] R. Carminati and J. J. Greffet, Phys. Rev. Lett. **82**, 1660 (1999).
[2] J. J. Greffet, R. Carminati, K. Joulain, J. P. Mulet, S. Mainguy, and Y. Chen, Nature (London) **416**, 61 (2002).
[3] M. Laroche, C. Arnold, F. Marquier, R. Carminati, J. J. Greffet, S. Collin, N. Bardou, and J. L. Pelouard, Opt. Lett. **30**, 2623 (2005).
[4] M. W. Tsai, T. H. Chuang, C. Y. Meng, Y. T. Chang, and S. C. Lee, Appl. Phys. Lett. **89**, 173116 (2006).
[5] Yves C. Martin, H. F. Hamann, and H. Kumar Wickramasinghe, J. Appl. Phys. **89**, 5774 (2001).
[6] G. Domingues, S. Volz, K. Joulain, and J. J. Greffet, Phys. Rev. Lett. **94**, 085901 (2005).
[7] M. Laroche, R. Carminat, and J. J. Greffet, J. Appl. Phys. **100**, 063704 (2006).
[8] K. Matsumoto, A. Inomata, and S. Hasegawa, Fujitsu Sci. Tech. J. **42**, 158 (2006).
[9] A. Cvitkovic, N. Ocelic, J. Aizpurua, R. Guckenberger, and R. Hillenbrand, Phys. Rev. Lett. **97**, 060801 (2006).
[10] E. Cubukcu, E. A. Kort, K. B. Crozier, and F. Capasso, Appl. Phys. Lett. **89**, 093120 (2006).

[11] J. Alda, J. M. Rico-Garcia, J. M. Lopez-Alonso, and G. Boreman, Nanotechnology **16**, S230 (2005).
[12] H. F. Hamann, A. Gallagher, and D. J. Nesbitt, Appl. Phys. Lett. **76**, 1953 (2000).
[13] L. Novotny, Phys. Rev. Lett. **98**, 266802 (2007).
[14] S. Ingvarsson, L. J. Klein, Y. Au, J. A. Lacey, and H. F. Hamann, Opt. Express **15**, 11249 (2007).
[15] H. F. Hamann, Proc. SPIE **5766**, 126 (2005).
[16] Y. de Wilde, F. Formanek, R. Carminati, B. Gralak, P. A. Lemoine, K. Joulain, J. P. Mulet, Y. Chen, and J. J. Greffet, Nature (London) **444**, 740 (2006).
[17] SiC provides a fairly good approximation to a blackbody within our spectral range of interest 2 to 5 μm, C. P. Cagran, L. M. Hanssen, M. Noorma, A. V. Gura, and S. N. Mekhontsev, Int. J. Thermophys. **28**, 581 (2007).
[18] H. F. Hamann, J. A. Lacey, and S. Ingvarsson, J. Microsc. **229**, 512 (2008).